# CHAPTER 14

# Comparison of Fluorine(18)-fluorodeoxyglucose and Gallium(68)-citrate PET/CT in patients with tuberculosis

Ankrah AO, Lawal IO, Boshomane TMG, KleinHC., Ebenhan T, RAJO, Vorster M, Glaudemans2 AWJM, Sathekge MM

**Nuklearmedizin 2019; 58:371-8**

## Abstract

$^{18}$F-FDG and $^{68}$Ga-citrate PET/CT have both been shown to be useful in the management of tuberculosis (TB). We compared the abnormal PET findings of $^{18}$F-FDG- and $^{68}$Ga-citrate-PET/CT in patients with TB.
**Methods**: Patients with TB on anti-TB therapy were included. Patients had a set of PET scans consisting of both $^{18}$F-FDG and $^{68}$Ga-citrate. Abnormal lesions were identified, and the two sets of scans were compared. The scan findings were correlated to the clinical data as provided by the attending physician.
**Results**: 46 PET/CT scans were performed in 18 patients, 11 (61%) were female, and the mean age was 35.7 ± 13.5 years. Five patients also had both studies for follow-up reasons during the use of anti-TB therapy. Thirteen patients were co-infected with HIV. $^{18}$F-FDG detected more lesions than $^{68}$Ga-citrate (261 vs. 166, $p<0.0001$). $^{68}$Ga-citrate showed a better definition of intracerebral lesions due to the absence of tracer uptake in the brain. The mean SUVmax was higher for $^{18}$F-FDG compared to $^{68}$Ga-citrate (5.73 vs. 3.01, $p< 0.0001$). We found a significant correlation between the SUVmax of lesions that were determined by both tracers ($r=0.4968$, $p<0.0001$).
**Conclusion**: Preliminary data shows $^{18}$F-FDG-PET detects more abnormal lesions in TB compared to $^{68}$Ga-citrate. However, $^{68}$Ga-citrate has better lesion definition in the brain and is therefore especially useful when intracranial TB is suspected.

## Introduction

Tuberculosis (TB) is the ninth leading cause of mortality worldwide. The incidence of TB for 2017 was estimated at 10 million, nine percent of these had a co-infection with human immune deficiency virus (HIV). Almost 1.7 million people with TB, including about 300,000 with a co-infection with HIV, died from TB in 2017 [1]. The diagnosis of TB is usually based on microscopic detection of acid-fast bacilli or more recently by the detection of nucleic acid sequences of *Mycobacterium tuberculosis* by polymerase chain reaction (PCR) from the sputum of patients with clinical signs and symptoms suggesting TB. Empiric anti-TB treatment is started at this stage with a sputum sample sent for culture and sensitivity. The results of the TB culture and sensitivity are not available until after treatment has already started. In extra-pulmonary TB (EPTB) diagnosis is often by the recovery of *Mycobacterium tuberculosis* by culture from a biopsy specimen taken from suspected site of infection. The standard methods currently used for TB diagnosis may be insufficient for early identification and prompt initiation of treatment that is crucial in the management of TB. The diagnosis of TB can be especially tricky when there is underlying HIV due to a higher incidence of smear-negative pulmonary TB (SNTB) and EPTB. The World Health Organization (WHO) has provided algorithms for the diagnosis of SNTB and EPTB in areas with high HIV prevalence or low resource settings. These WHO algorithms have been validated and incorporated in the National TB guidelines of many affected countries [2-6]. WHO recommends that all available tools must be deployed to combat the TB pandemic [7]. PET/CT has demonstrated several valuable applications in the management of TB. $^{18}$F-FDG-PET/CT may help in diagnosing TB by identifying a suitable biopsy site, determining the extent of involvement, evaluating treatment response, and providing real-time assessment of disease burden. $^{18}$F-FDG-PET/CT is particularly helpful in the management of patients with SNTB and EPTB [8]. Various other PET tracers have also been evaluated for different indications in TB [9] with a recent growing interest in Gallium 68 ($^{68}$Ga) based radiopharmaceuticals [10]. This interest is due to the availability of Germanium-68/Gallium-68 generator ($^{68}$Ge/$^{68}$Ga-generators) that ensures a readily available source of the PET radionuclide $^{68}$Ga for almost 24 hours in a day, for about one year [11]. Therefore, and unlike $^{18}$F-FDG, $^{68}$Ga-citrate does not require a cyclotron, no special patient preparation is needed, and the radiolabeling is relatively easy. Despite these advantages of $^{68}$Ga-citrate, some disadvantages exist compared to $^{18}$F-FDG. The tracer is not as widely available as $^{18}$F-FDG and has not been validated in many diseases. The physical properties of $^{18}$F are more favorable for clinical PET imaging than those of $^{68}$Ga. Despite the disadvantages, $^{68}$Ga-citrate has shown promise in some infections, including TB [12-14]. In TB, $^{18}$F-FDG lesions are visualized due to the increased glucose utilization by activated immune cells. $^{68}$Ga-citrate uptake in TB is due to both specific and non-specific mechanisms, including the increased vascular permeability, and the uptake by iron-binding proteins such as transferrin and siderophores [10]. No head-to-head comparison has been made to compare $^{18}$F-FDG and $^{68}$Ga-citrate tracer uptake in patients with TB directly on PET/CT. The aim of the study was to compare the abnormal tracer uptake of $^{18}$F-FDG and $^{68}$Ga-citrate PET/CT directly in patients with TB at different time-points during anti-TB treatment.



## Methodology

Eighteen patients with TB were included in the study. We included patients that had microscopic, PCR, or culture evidence of TB. We also included patients who had SNTB or EPTB and met the WHO criteria for the diagnosis of TB [5]. They all underwent a $^{68}$Ga-citrate PET/CT and $^{18}$F-FDG PET/CT at least 24 hours apart but within two weeks and in no specific order. We recruited the patients from the Steve

Biko Academic Hospital, a tertiary referral center in Pretoria, South Africa. We retrieved microbiology and pathology data from electronic laboratory database to determine how the diagnosis of TB was settled. We also documented whether the patient had a co-infection of HIV, and recorded the viral load and the CD4 count if an HIV co-infection existed. The attending physicians of the patients were contacted for the outcome in patients when follow-up data were required for the study. The institutional review board approved the study with ethics reference number 430/2016. All patients who participated in the study signed an informed consent form. We excluded patients under 18 years of age, pregnant women, lactating mothers, and patients who could not consent. We included TB patients at different time points during their treatment with anti-TB medication to compare the performance of tracers at different stages during the anti-TB therapy. Five of the patients who had baseline scans also had follow-up scans with both tracers during the course of their treatment. We defined a baseline study as a scan in a patient who had not received more than two weeks of anti-TB treatment. The response to therapy was assessed by comparing the percentage change of the mean lesion to liver SUVmax ratio of both tracers.

### $^{18}$F-FDG PET/CT

Patients were scanned according to the international guidelines. We asked patients to fast for at least 6 hours, and patients were scanned if their blood glucose was less than 10mmol/L. The activity of $^{18}$F-FDG injected for each patient was based on his or her body weight, calculated by the formula; [(body weight in kg ÷ 10) +1] X 37MBq. The mean circulation time after injection of $^{18}$F-FDG was 67.5 ± 4.42 minutes, and the mean activity of $^{18}$F-FDG injected was 255.3 ± 44.4 MBq. PET images were acquired on an integrated PET/CT camera system (Biograph mCT 40 slice, Siemens Medical Solution, IL, USA). Whole-body scan from mid-thigh to the vertex of the skull was acquired with 3 minutes per bed position at one hour after injection of $^{18}$F-FDG. Diagnostic contrast-enhanced CT was performed adjusted for the patient's weight: tube voltage of 120kV, tube –current product 40-150 mAs with an online tube current modulation section width of 5mm and pitch factor of 0.8. CT images were enhanced with 100 ml of intravenous non-ionic contrast (GE Healthcare WI, USA). CT images were used for attenuation correction and anatomic localization.

### $^{68}$Ga-citrate preparation

$^{68}$Ga-citrate was prepared using compounded radiolabeling of $^{68}$Ga-citrate with radioactivity eluted from a $SnO_2$-based $^{68}$Ge/$^{68}$Ga-generator (iThemba LABS, Somerset West, South Africa) [15]. Briefly, $^{68}GaCl_3$ yielded in 1-2 mL by eluate fractionation in 10 ml of 0.6 N hydrochloric acid, was added to directly to a vial containing anticoagulant citrate dextrose solution, USP formula A (ACD-A) in a one-step-aseptic procedure, incubated for 15-20 minutes with frequent vortexing. This method was based on a combination of the two previous protocols [13, 16]. All solvents used were of a pharmacological grade. Quality control was performed before $^{68}$Ga-citrate injection, including instant thin-layer chromatography and determination of the pH value.

### $^{68}$Ga-citrate PET/CT imaging

Patients were not required to fast before the study. Patients were injected with a mean activity of 140.2 ± 41.1 MBq of $^{68}$Ga-citrate and mid-thigh to the vertex of skull images were acquired on the same PET/CT system used for the $^{18}$F-FDG studies. The mean circulating time after injection of the $^{68}$Ga-citrate was 64.95 ± 5.3 minutes. The acquisition was 4 minutes per bed position, and a low dose non-

contrasted CT was used for attenuation correction (tube voltage of 120kV, tube–current product 40-50 mAs with a pitch factor of 1.5).

### Image reconstruction and interpretation

PET images were reconstructed with and without CT based attenuation correction using ordered-subset expectation maximum and displayed as axial, sagittal, and coronal slices. Two nuclear physicians (AA and IL) who were aware of the patient's diagnosis of TB and their HIV status were asked to assess both the $^{18}$F-FDG and $^{68}$Ga-citrate for sites of abnormal uptake. Sites of abnormal tracer uptake were noted, and we recorded lesions showing uptake of one tracer but not the other. Any differences were resolved by a third nuclear physician (MM) and correlated with anatomical data that had been reported by a board-certified radiologist.

### PET analysis

After determining the sites of abnormal tracer uptake, AO drew the volume of interest (VOI) for each lesion. The SUVmax for each any abnormal lesion detected by either of the tracers was recorded. In patients with follow-up scans, the baseline study was compared to the follow-up study for $^{18}$F-FDG and $^{68}$Ga-citrate. We calculated and compared the mean change in SUVmax of the lesion to the liver ratio from baseline to follow up for the two tracers.

### Statistical analysis

We used SPSS Version 23 for the statistical analysis. We used descriptive statistic to describe parameters such as the age, duration of treatment, and SUVmax of lesions. We used the Chi-squared test to determine the significance of the difference in the number of lesions detected by each tracer. The paired Students *t*-test was used to determine the significance of the difference in means SUV of the two tracers; the Cohen Kappa test was used to assess the agreement between $^{18}$F-FDG and $^{68}$Ga-citrate PET/CT in the detection of lesions and follow-up in TB patients. The Pearson correlation coefficient was used to determine the association between the SUVmax of lesions detected by both $^{18}$F-FDG and $^{68}$Ga-citrate.

## Results

Finally, 18 patients received 46 PET/CT scans, 23 pairs of PET/CT studies: 23 $^{18}$F-FDG, and 23 $^{68}$Ga-citrate PET/CT studies. The mean age of the patients was 35.7 ± 13.5 years, and 7 (39%) were males. The patient demographics and HIV parameters are summarized in Table 1.

### Duration of anti-TB treatment before the scan and interval between scans

Six scan pairs were done within one week of initiation of anti-TB therapy; seven were done at two weeks, five scans were done at eight weeks, one pair each was done at nine weeks, ten weeks, 26 weeks, 39 weeks and 52 weeks after starting anti-TB therapy. The interval between the $^{18}$F-FDG and $^{68}$Ga-citrate PET/CT studies for each scan pair has been tabulated in Table 2 below.

**Table 1: Patient demographic data and HIV parameters**

| | |
|---|---|
| Patients (n) | 18 |
| Sex (female, n) | 11 (61.1%) |
| Age (years, mean) | 35.67 ± 13.53 |
| HIV patients (n) | 13 (72.2%) |
| CD4 count (median) | 198 (32-1,008) |
| Viral load (median) | 66 (0- 232,916) |

**Table 2: Interval between $^{18}$F-FDG and $^{68}$Ga-citrate studies**

| Interval between scan pairs in days | Number of scan pairs | Percentage of scan pairs (%) | Cumulative percentage (%) |
|---|---|---|---|
| 1 | 2 | 9 | 9 |
| 2 | 4 | 17 | 26 |
| 4 | 6 | 26 | 52 |
| 5 | 5 | 22 | 74 |
| 6 | 3 | 13 | 87 |
| 8 | 2 | 9 | 96 |
| 12 | 1 | 4 | 100 |

## Diagnosis of TB and HIV co-infection

Twelve (67%) patients had their TB diagnosis confirmed by biopsy and culture or polymerase chain reaction (PCR) of the sputum. In six patients (33%), the diagnosis was per the WHO algorithm and National guidelines for the diagnosis and follow-up of SNTB and EPTB in an HIV-prevalent setting [2, 4]. Table 3 shows how the diagnosis of TB was established. Thirteen patients (72%) were co-infected with HIV. The median CD4 count and viral load of TB/HIV patients were 198 (range 32-1,008) and 66 (range 0-232,918), respectively.

## Lesions

In total, we counted 269 different lesions from both tracers. $^{18}$F-FDG detected 269 (97%) and $^{68}$Ga-citrate detected 166 (62%) lesions, $p< 0.0001$. We found pulmonary involvement in 12 patients (67%), nodal involvement in 13 (72%), and pleural involvement in 3 (17%) of the patients. Other sites of abnormal tracer uptake included the brain, spleen, liver, vertebrae and disc, skin, subcutaneous tissue, and joints (Table 4) The mean SUVmax of the lesions detected was higher for $^{18}$F-FDG (5.73 ± 3.05) than the SUVmax for $^{68}$Ga-citrate (3.01 ± 1.31) $p< 0.0001$.

## Comparison of $^{18}$F-FDG and $^{68}$Ga-citrate PET/CT findings in patients

We present the findings of the head-to-head tracer comparison in Table 5. We also depict the correlation of the SUVmax of $^{68}$Ga-citrate and $^{18}$F-FDG in lesions in Figure 1. There was a significant correlation between the SUVmax of the lesions that were detected by both $^{18}$F-FDG and $^{68}$Ga-citrate. We noted complete concordance of all abnormal lesions in five patients (27.7%). Eleven patients (55.6%) had more lesions detected on $^{18}$F-FDG-PET/CT. The lesions that were seen on $^{18}$F-FDG and not on $^{68}$Ga-citrate were usually located near the mediastinum and large vessels where the blood pool from $^{68}$Ga-citrate made it difficult to discriminate the pathological uptake from the background.

Furthermore, pericarditis was identified on $^{18}$F-FDG but could not on the $^{68}$Ga-citrate due to the uptake of $^{68}$Ga-citrate the cardiac blood pool.

**Table 3: Diagnosis of TB**

| Diagnosis of TB | |
|---|---|
| Microscopically confirmed (n) | 12 (66.7%) |
| Biopsy and culture (n) | 3 |
| Sputum polymerase chain reaction only | 4 |
| Sputum polymerase chain reaction and subsequent growth by culture | 4 |
| Sputum culture only | 1 |
| Clinical and follow up as per WHO algorithm for EPTB and SNTB (n) | 6 (33.3%) |
| Extra-pulmonary tuberculosis only | 1 |
| Smear-negative tuberculosis | 5 |

**Table 4: Sites of abnormal lesions detected by $^{18}$F-FDG and $^{68}$Ga-citrate**

| Site | Number of patients (%) |
|---|---|
| Lungs[1] | 12 (67) |
| Lymph nodes[1*] | 13 (72) |
| Pleura[1] | 2 (11) |
| Skin[1] | 1 (5) |
| Liver[1*] | 1 (5) |
| Spleen[1] | 1 (5) |
| Joint [1] | 1 (5) |
| Subcutaneous tissue[1] | 1 (5) |
| Vertebrae and disc[2±] | 1 (5) |
| Pericardium[2] | 1 (5) |
| Brain[1#] | 1 (5) |

[1] Lesions detected by both $^{18}$F-FDG and $^{68}$Ga-citrate

[2] Lesions detected by $^{18}$F-FDG only

[*] Lower number lesions on $^{68}$Ga-citrate

[±] Low uptake of $^{18}$F-FDG in assessment of residual TB

[#]More clearly defined on $^{68}$Ga-citrate

**Table 5: Head-to-head comparison of $^{18}$F-FDG- and $^{68}$Ga-citrate-PET/CT findings**

| Abnormal uptake | N (%) | Comment |
|---|---|---|
| Concordance of all lesions | 5 (27.7) | Four out of five cases were in HIV-negative patients. |
| More lesions on [$^{18}$F]FDG | 11 (61.1) | Includes one patient who had TB-pericarditis, which was only visualized on $^{18}$F-FDG-PET/CT. Most of the other lesions were lymph nodes. |
| Better defined on $^{68}$Ga-citrate | 1 (5.6) | Both tracers detected larger brain abscesses. Smaller ones were only detected by $^{68}$Ga-citrate |
| Suspected residual disease | 1 (5.6) | After one year of anti-TB, there was an equivocal uptake on the $^{18}$F-FDG with no uptake on $^{68}$Ga-citrate. No further anti-TB was administered and clinical follow-up and an MRI 3 months later confirmed no residual TB |

Concordant – all lesions detected by $^{18}$F-FDG were also detected by $^{68}$Ga-citrate

**Figure 1**

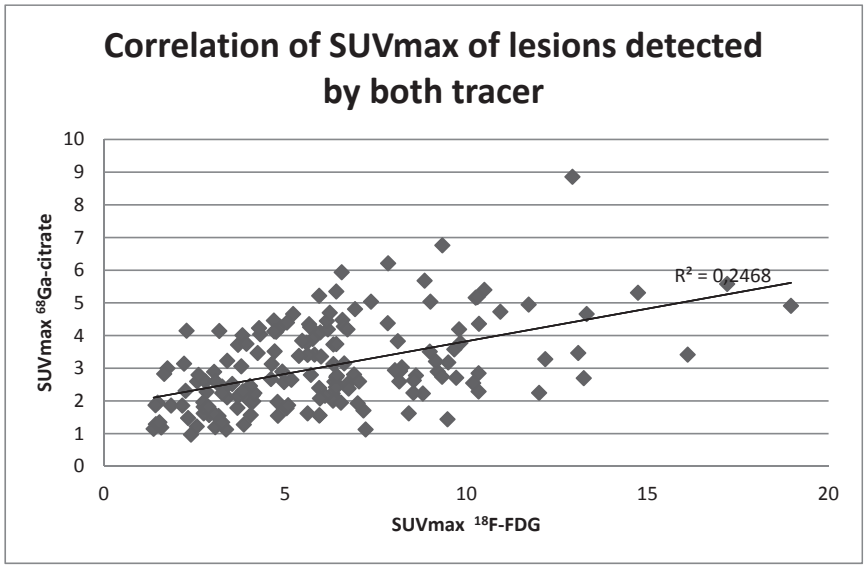


$R^2$ 0.2468, *P* >0.0001

Conversely, in one patient, $^{68}$Ga-citrate showed better lesion definition of intracerebral lesions with better lesion-to-background ratio compared to the $^{18}$F-FDG studies with its inherently high level of background activity in the brain. The intracerebral lesions were better visualized on the $^{68}$Ga-citrate study (Figure 2). In the last patient, there was $^{18}$F-FDG uptake but not $^{68}$Ga-citrate in a patient who had completed anti-TB treatment and was for assessment of residual disease in the spine.

Using Cohen kappa analysis for the detection of abnormal tracer uptake in TB patients, we found substantial agreement between the two tracers in detection abnormal lesions in patients with TB (kappa 0.64).

$^{18}$F-FDG was unable to exclude residual disease in TB spondylodiscitis in a patient where $^{68}$Ga-citrate was negative, in a patient who was determined to have no residual TB by clinical follow-up after a year of PET/CT scan with no anti-TB therapy. Also, $^{68}$Ga-citrate did not accumulate in an inflammatory lesion due to healed post-staphylococcal abscess in a patient who had histologically confirmed TB arthritis of the right knee (Figure 3).

**Figure 2** Transverse PET, CT, and fused PET/CT images $^{18}$F-FDG (left) and $^{68}$Ga-citrate (right) of a patient with intracerebral TB with a better definition of the lesion on the $^{68}$Ga-citrate image. The lesion can barely be visualized on the [$^{18}$F]FDG PET image only. The CT component of [F]FDG-PET/CT was contrast enhanced.

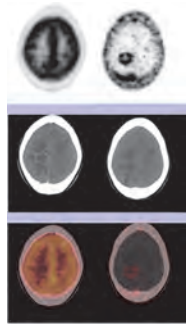

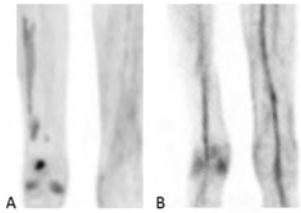


**Figure 3** A. $^{18}$F-FDG and B. $^{6}$Ga-citrate MIP images of the thighs and knees bilaterally of a 26-year-old male with microbiologically proven TB arthritis of the right knee. $^{18}$F-FDG shows post-infective inflammation not taken up by $^{68}$Ga-citrate in the lateral compartment of the right thigh. The patient had culture-confirmed staphylococcal abscesses two months before the PET/CT studies that had been successfully treated with antibiotics.

### Follow-up

All our patients received first-line anti-TB drugs for the treatment of TB. We repeated the scans in five patients, all of whom had baseline studies. Four patients had their scans repeated after eight weeks of first-line anti-TB therapy and one patient after twenty-six week of first-line anti-TB therapy. In all five patients, both tracers showed a decreasing mean lesion to liver SUVmax ratio by both tracers in response to the anti-TB treatment (Table 6). In all five patients, the decreasing lesion to liver ratio of SUVmax of both tracers with anti-TB treatment was consistent with the clinical outcome of the patients as indicated by their clinicians (measured by patient symptoms, weight, hemoglobin concentration changes, CRP and ESR). The percentage change for the mean lesion to liver SUVmax of the lesions in patients that had follow-up studies ranged from -95.2% to -33.6% for $^{18}$F-FDG while that of $^{68}$Ga-citrate ranged from -85% to -43.1% (Table 6).

**Table 6: Percentage change in mean target to liver SUVmax ratio of abnormal lesions in patient who had follow-up studies**

| | Site of lesion | $^{18}$F-FDG | $^{68}$Ga-citrate |
|---|---|---|---|
| **Patient A** | Lung and nodes | -33.6% | -47.5% |
| **Patient B** | Lung | -95.2% | -85% |
| **Patient C** | Nodes | -40.4% | -43.1% |
| **Patient D** | Nodes | -35.7% | -70.3% |
| **Patient E** | Brain, Lung | -70% | -63.4% |

## Discussion

In this first head-to-head comparison of $^{18}$F-FDG and $^{68}$Ga-citrate PET/CT in patients with TB, we found more abnormal lesions were detected by $^{18}$F-FDG but better lesion definition by $^{68}$Ga-citrate for intracranial lesions. Our study also suggested that $^{68}$Ga-citrate was less likely to accumulate in post-infective inflammation compared to $^{18}$F-FDG.

$^{68}$Ga-citrate, as a PET tracer, is particularly attractive to facilities that have no on-site cyclotron as the radionuclide, $^{68}$Ga, is readily available in-house from good manufacturing practice (GMP) approved $^{68}$Ga generators. The radiopharmaceutical is also easy to prepare, without the need for highly skilled radiopharmacist and technical staff needed to operate a cyclotron.

The management of TB can be challenging, especially in SNTB and EPTB, particularly in areas with a high prevalence of HIV. Imaging becomes very critical in the management of such cases. PET/CT has been found to be useful in the management of these complex TB cases [17]. The use of $^{68}$Ga-citrate

PET/CT to manage TB may be a particularly attractive prospect to developing economies with a high TB burden, where efforts are in place to increase the use of nuclear medicine [18].

Intracranial TB is associated with higher mortality rates than other forms of TB [19]. Objective assessment of therapy to guide clinicians in the management is essential [20]. The ability of PET to quantify disease burden using semi-quantitative indices makes it a particularly useful imaging technique for monitoring therapy. The application of $^{18}$F-FDG, the most commonly used PET tracer, is limited in intracerebral lesions because of significant physiologic brain uptake [17]. $^{68}$Ga-citrate does not show physiologic tracer accumulation in the brain. Lesions in the brain can be detected with a high contrast resolution. Like $^{18}$F-FDG, $^{68}$Ga-citrate is a nonspecific tracer. $^{68}$Ga-citrate does not only accumulate in TB but also in other conditions such as malignancy [21]. The role of $^{68}$Ga-citrate in intracerebral lesions may not be limited to TB, but may also apply to other intracranial pathologies where $^{18}$F-FDG has a poor clinical record in their management.

Our study suggests $^{68}$Ga-citrate is less likely to accumulate in post-infective inflammation. This may become an important clinical application, especially since $^{18}$F-FDG is known to persist in some TB lesions even after treatment [22]. More extensive studies will be required to investigate this role of $^{68}$Ga-citrate further.

The use of PET/CT in the evaluation of a co-infection of TB and HIV can be challenging. HIV-associated lymphadenopathy is known to be $^{18}$F-FDG avid [23]. Treatment with antiretroviral and stage of HIV infection may influence the metabolic $^{18}$F-FDG signal in the lymph nodes. Although $^{68}$Ga-citrate is a non-specific tracer, there is currently no study to determine the uptake of $^{68}$Ga-citrate in HIV-associated lymphadenopathy. Again, $^{68}$Ga-citrate has not been as extensively studied in HIV-associated infection and malignancies as $^{18}$F-FDG. In our study, we had over 70% of our patients with HIV. These patients had no clinical evidence of an alternative diagnosis such as HIV-associated malignancies at time of study and up to 2 years of follow up. The differences in the uptake and number of lesions detected by $^{18}$F-FDG and $^{68}$Ga-citrate are likely due to the differences in the mechanism of uptake and normal tracer biodistribution. The difference may also be related to differential uptake by the tracers in HIV-lymphadenopathy.

The findings from $^{18}$F-FDG and $^{68}$Ga-citrate would, in most cases (except for two), not have resulted in alteration of the treatment based on differences in PET/CT findings despite $^{18}$F-FDG detecting more lesions. The standard treatment that is given to the patients with pulmonary TB or TB lymphadenitis susceptible to first-line therapy is six months on anti-TB drugs, so the additional lymph nodes detected by $^{18}$F-FDG PET/CT would not have potentially altered the TB management. In two patients, however, the results of the PET/CT scans would have led to different management strategies. In the patient with pericarditis, the abnormal $^{18}$F-FDG uptake in the pericardium (not visualized on $^{68}$Ga-citrate) was considered to be TB pericarditis and led to a prolongation of anti-TB therapy to nine months instead of the standard six months used for pulmonary and nodal disease. In the patient who was assessed for residual TB spondylodiscitis, $^{18}$F-FDG was unable to exclude residual TB convincingly, but lack of $^{68}$Ga-citrate uptake suggested no residual disease; in this case, $^{68}$Ga-citrate potentially led to the correct treatment as it corresponded to the clinical strategy adopted by clinicians and was proven to be correct by clinical follow-up. Our study suggests $^{68}$Ga-citrate PET/CT may detect the abnormal TB lesions detected by $^{18}$F-FDG PET/CT however in special cases one tracer may have benefits over the other such as intracerebral lesions for $^{68}$Ga-citrate PET/CT or pericarditis for $^{18}$F-FDG PET/CT.

This is the first study comparing the role of $^{18}$F-FDG and $^{68}$Ga-citrate in TB patients. In a previous clinical study, the role of $^{68}$Ga-citrate was compared to $^{18}$F-FDG in patients with an infectious process, and the two were found to be comparable in the detection of staphylococcal osteomyelitis [24]. The authors found the SUVmax of soft tissue lesions with $^{68}$Ga-citrate to be less than with $^{18}$F-FDG, which is similar to our findings. The higher SUV of the $^{18}$F-FDG lesions are due to the better physical properties of $^{18}$F and led to a better definition of the abnormal lesions at most sites except in the brain. Despite this, our study showed that $^{68}$Ga-citrate-PET/CT detected abnormal tracer uptake in all the patients who had TB. Another study evaluated the characteristics of $^{18}$F-FDG and $^{68}$Ga-citrate PET/CT in a condition characterized by a severe inflammatory process with necrosis due to the reaction to metal debris in patients with metal on metal hip arthroplasties [25]. $^{18}$F-FDG PET/CT showed periprosthetic uptake in 94% (15/16) of hip arthroplasties with $^{68}$Ga-citrate showing periprosthetic uptake in only 19% (3/16). The three hips that showed abnormal uptake on $^{68}$Ga-citrate were the same hips that the pattern of uptake on $^{18}$F-FDG PET/CT was suggestive of an infection, although infection was confirmed in only one hip. These findings are consistent with our finding that $^{68}$Ga-citrate is less likely to accumulate in inflammatory lesions with no active infection compared to $^{18}$F-FDG. Again, a more recent study found $^{68}$Ga-citrate was more specific than $^{18}$F-FDG in distinguishing infected lower limb prosthesis from sterile inflammation [26]. This critical role must be explored further due to the limited number of post-infective lesions we had in our study.

Our study has some limitations. It has a small sample size, the differences in anti-TB treatment duration, time between $^{18}$F-FDG and $^{68}$Ga-citrate studies. Again, although all patients had sufficient clinical data for follow-up as per international and national algorithms, histology could not be done on all patients as biopsy was not always possible. The activity injected for $^{68}$Ga-citrate has not yet been standardized.

The duration between the $^{18}$F-FDG and $^{68}$Ga-citrate was variable but less than 12 days with more than 85% (20 out of the 23) done by six days (Table 3). *Mycobacterium tuberculosis* is a relatively slow-growing organism with the treatment of active disease lasting at least six months. The duration of fewer than two weeks between the $^{18}$F-FDG and $^{68}$Ga-citrate is unlikely to change the tracer uptake significantly.

Large prospective studies evaluating the role of a more homogenous population such as patients with suspected residual disease TB spondylodiscitis or intracerebral TB will be needed to fully exploit the potential advantages offered by $^{68}$Ga-citrate PET/CT in the management of TB. The role of $^{68}$Ga-citrate in non-TB bacterial infection and other granulomatous processes with high $^{18}$F-FDG uptake must be investigated further.

## Conclusion

Our preliminary data shows that $^{18}$F-FDG detects more abnormal lesions than $^{68}$Ga-citrate in patients being managed for tuberculosis. However, $^{68}$Ga-citrate has better lesion definition of intracranial lesions and may be especially indicated for such lesions. The study provides data and a basis for large multicenter prospective studies of the use of $^{68}$Ga-citrate in TB.



### Disclosure

The authors report no conflict of interest relevant to this article.

**Acknowledgments**

The authors wish to acknowledge all the staff of the Nuclear Medicine department of the Steve Biko Academic Hospital and patients who consented to be part of the study

**Conflict of interest**

The authors declare there is no conflict of interest.

## References


1. Global tuberculosis report 2018. Geneva: World Health Organization; 2018. http://apps.who.int/iris/bitstream/handle/10665/274453/9789241565646-eng.pdf Assessed January 18, 2019.
2. Improving the diagnosis and treatment for smear-negative pulmonary and extrapulmonary tuberculosis among adults and adolescents. Recommendations for HIV-prevalent and resource-constrained settings. WHO 2007, http://apps.who.int/iris/bitstream/handle/10665/69463/WHO_HTM_TB_2007.379_eng.pdf;jsessionid=244682331B1F968F813FD965BF270051?sequence=1 Assessed January 18, 2019.
3. **Wilson D, Mbhele L, Badri M, et al.** Evaluation of the World Health Organization algorithm for the diagnosis of HIV-associated sputum smear-negative tuberculosis. Int J Tuberc Lung Dis. 2011; 15:919-24.
4. Department of Health, Republic of South Africa. National Tuberculosis Management Guidelines, Department of Health, South Africa 2014 http://www.tbonline.info/media/uploads/documents/ntcp_adult_tb-guidelines-27.5.2014.pdf Assessed 18 January 2019.
5. **Walley J, Kunutsor S, Evans M, et al.** Validation in Uganda of the new WHO diagnostic algorithm for smear-negative pulmonary tuberculosis in HIV prevalent settings. J Acquir Immune Defic Syndr. 2011; 57:e93-100.
6. **Linguissi LS, Vouvoungui CJ, Poulain P, et al**. Diagnosis of smear-negative pulmonary tuberculosis based on clinical signs in the Republic of Congo. BMC Res Notes. 2015; 8:804.
7. The Stop TB Strategy.WHO *www.who.int/tb/strategy/stop_tb_strategy/en/* Accessed August 4, 2018.
8. **Sathekge M, Maes A, Van de Wiele C.** FDG-PET imaging in HIV infection and tuberculosis. Semin Nucl Med. 2013; 43:349-66.
9. **Ankrah AO, van der Werf TS, de Vries EF, et al**. PET/CT imaging of Mycobacterium tuberculosis infection. Clin Transl Imaging. 2016; 4:131-44.
10. **Banerjee SR, Pomper MG.** Clinical Applications of Gallium-68. Appl Radiat Isot. 2013; 0:2-13.
11. **Vorster M, Maes A, Wiele Cv, et a**l. Gallium-68 PET: A Powerful Generator-based Alternative to Infection and Inflammation Imaging. Semin Nucl Med. 2016; 46:436-47.
12. **Nanni C, Errani C, Boriani L, et al.** $^{68}$Ga-citrate PET/CT for evaluating patients with infections of the bone: preliminary results. J Nucl Med. 2010;51:1932-6.
13. **Kumar V, Boddeti DK, Evans SG, et a**l. $^{(68)}$Ga-Citrate-PET for diagnostic imaging of infection in rats and for intra-abdominal infection in a patient. Curr Radiopharm. 2012; 5:71-5.
14. **Vorster M, Maes A, Van de Wiele C, et al.** 68Ga-citrate PET/CT in Tuberculosis: A pilot study. Q J Nucl Med Mol Imaging. 2019; 63:48-55.
15. **Vorster M, Mokaleng B, Sathekge MM, et al.** A modified technique for efficient radiolabeling of 68Ga-citrate from a SnO2-based 68Ge/68Ga generator for better infection imaging. Hell J Nucl Med. 2013; 16:193-198.
16. **Rizzello A, Di Pierro D, Lodi F, et al.** Synthesis and quality control of $^{68}$Ga citrate for routine clinical PET. Nucl Med Commun. 2009; 30:542-5.
17. **Ankrah AO, Glaudemans AWJM, Maes A, et al**. Tuberculosis. Semin Nucl Med. 2018; 48:108-30.
18. **Dondi M, Kashyap R, Paez D, et al.** Trends in nuclear medicine in developing countries. J Nucl Med. 2011; 52:16S-23S.
19. **El Sahly HM, Teeter LD, Pan X, et al.** Mortality Associated with Central Nervous System Tuberculosis. The Journal of infection. 2007; 55:502-509.

20. **Torres C, Riascos R, Figueroa R, et al.** Central nervous system tuberculosis. Top Magn Reson Imaging. 2014; 23:173-89.
21. **Malherbe ST, Shenai S, Ronacher K, et al.** Persisting positron emission tomography lesion activity and Mycobacterium tuberculosis mRNA after tuberculosis cure. Nat Med. 2016; 22:1094-100.
22. **Vorster M, Maes A, Jacobs A, et al.** Evaluating the possible role of 68Ga-citrate PET/CT in the characterization of indeterminate lung lesions. Ann Nucl Med. 2014; 28:523-30.
23. **Lucignani G, Orunesu E, Cesari M, et al.** FDG-PET imaging in HIV-infected subjects: relation with therapy and immunovirological variables. Eur J Nucl Med Mol Imaging. 2009; 36:640-47.
24. **Salomäki SP, Kemppainen J, Hohenthal U, at al.** Head-to-Head Comparison of 68Ga-Citrate and 18F-FDG PET/CT for Detection of Infectious Foci in Patients with Staphylococcus aureus Bacteraemia. Contrast Media Mol Imaging. 2017; 2017:3179607.
25. **Aro E, Seppänen M, Mäkelä KT, et al.** PET/CT to detect adverse reactions to metal debris in patients with metal-on-metal hip arthroplasty: an exploratory prospective study. Clin Physiol Funct Imaging. 2018; 38:847-55
26. **Tseng JR, Chang YH, Yang LY, et al**. Potential usefulness of 68Ga-citrate PET/CT in detecting infected lower limb prostheses. EJNMMI Res. 2019; 9:2